Pilot Tone Signal Optimization for Cardiac Magnetic Resonance Imaging

Undergraduate Honors Thesis

Submitted to the Department of Electrical and Computer Engineering in Partial Fulfillment of the Requirements for the Graduation with Honors Research Distinction at The Ohio State University

By

Abhishek Vijaykumar

Undergraduate Program in Electrical and Computer Engineering

The Ohio State University

2021

Thesis Committee

Dr. Rizwan Ahmad, Advisor

Dr. Orlando Simonetti

Abstract

Pilot Tone (PT) is an emerging technology in the field of cardiac magnetic resonance imaging (MRI). Its ability to effectively encode physiological motions has made it an attractive choice for cardiac MRI, where respiratory and cardiac motions are invariably present. PT is advantageous in cardiac MRI because of its high sampling rate and its ability to simultaneously encode cardiac and respiratory motions without interrupting the acquisition process. Typically, the cardiac signal extracted from PT data is of good quality; however, PT data can be excessively noisy and susceptible to electromagnetic interference and bulk motion artifact. To increase the robustness and reliability of the extracted cardiac signal from the PT data, it is imperative to enhance and optimize the data processing procedure.

This thesis focuses on the optimization of cardiac signal extraction and explores the hypothesis that by constructing bandwidth-optimized synthetic (BOSyn) channels from the measured raw PT data, the quality of the extracted cardiac signal can be significantly improved. By localizing the cardiac motion energy in the first few synthetic channels, BOSyn provides an avenue to perform channel pruning. These synthetic channels are generated from a linear combination of the measured PT channels. The weights that combine the measured PT channels into synthetic channels maximize the ratio of energy in the cardiac frequency range, called region-of-interest (ROI), to the

energy outside the ROI. The synthetic channels from BOSyn are sorted, with the first synthetic channel representing the highest relative energy in the ROI. After this procedure, the synthetic channels with small relative energy in the ROI are discarded to improve signal quality. The resulting synthetic channels can be processed further for cardiac motion extraction.

A study performed on 14 healthy volunteers' PT data, with electrocardiogram (ECG) data as reference, highlights the merit of the BOSyn-based channel pruning for cardiac motion extraction. In summary, the proposed method was effective in improving the accuracy and precision of the extracted cardiac triggers.

Dedication

I dedicate my thesis to my family and friends who have shown me immense support. A special thanks to my parents for their love and encouragement.

Acknowledgments

I would like to thank Dr. Rizwan Ahmad for giving me the opportunity to pursue this undergraduate research in the field of cardiac MRI. I am grateful for having the continuous support of Dr. Ahmad and Aaron Pruitt throughout the journey of conducting this research. The weekly meetings organized with Dr. Ahmad and Aaron proved to be extremely helpful in developing my interest in this field of research.

I thoroughly enjoyed this learning experience and have gained immense exposure in the field of academic research as well as writing and publishing.

Most importantly, I would like to thank my friends and family who have pushed me to persevere despite the ongoing pandemic. Without their love and support, this would not have been possible.

Vita

2017 to 2021.....B.S. Electrical and Computer Engineering, The Ohio State University

2021 to Present .....M.S. Electrical and Computer Engineering, The Ohio State University

Fields of Study

Major Field: Electrical and Computer Engineering

Table of Contents

List of Tables

List of Figures

Chapter 1. Introduction

1.1 Cardiac Magnetic Resonance Imaging and its Applications

Magnetic resonance imaging (MRI) utilizes powerful magnetic fields and radio waves to noninvasively create images of organs and tissues. Generally, an MRI exam includes several runs or sequences, which makes the image acquisition an inherently slow process. The quality of acquired images directly depends on the patient's ability to remain still during this long process. Cardiac MRI is a specific application of MRI that deals with detailed imaging of the areas within and around the heart. It serves as a tool to detect or monitor cardiac diseases and evaluate or monitor the heart's functionality and anatomy. Images obtained from cardiac MRI enable doctors to help diagnose problems related to the heart like coronary artery disease, cardiomyopathy, and heart valve disease. Therefore, it is imperative that the resulting images from a cardiac MRI scan are of diagnostic quality.

1.2 Standard Cardiac MRI Setup and its Challenges

1.2.1 Setup

Cardiac MRI is a more challenging application of MRI because it involves imaging an organ that is in a constant state of motion. The heart's periodic motion, as well as respiratory and bulk motion, make it quite challenging to obtain a detailed image of the heart [1]. Since the slow acquisition of MRI does not allow collecting all the required data in one heartbeat, the

acquisition is spread across multiple heartbeats. Traditional cardiac MRI techniques rely heavily on synchronization of the data acquisition with the cardiac and respiratory motion for artifact-free imaging.

In a traditional cardiac MRI setup, an electrocardiogram (ECG) provides real-time tracking of the cardiac motion. The MRI acquisition is synchronized with the ECG signal to capture data over many cardiac cycles. The data samples from multiple cardiac cycles are then aggregated to recover one high-quality beat. The synchronization is commonly based on R-wave detection because the R-wave can be reliably extracted from ECG data.

For respiratory motion compensation, different techniques are implemented like breath-holding, respiratory bellows, and navigator echoes. Breath-holding is the most commonly used strategy in practice as it can eliminate respiratory motion. Respiratory bellows use pressure sensors to directly measure chest expansion. A more widely used approach for respiratory motion synchronization is navigator echoes which detect the position of the diaphragm during respiration.

1.2.2 Challenges with Cardiac Motion Synchronization

For a successful ECG setup and monitoring for cardiac MRI, the patient undergoes the time-consuming process of electrode placement and, in some cases, shaving or clipping of chest hair. Most often, abrasive gels are used for skin cleaning to enable careful electrode placement. Cardiac motion synchronization using ECG in higher magnetic fields can be challenging. A stronger magnetic field produces a stronger MRI signal and, thus, better image quality. However, at magnetic fields of 3 Tesla or higher, the quality of ECG can be compromised due to the

motion of the conducting fluid (blood) in the magnetic field, also known as the magnetohydrodynamic effect or MHD [2]. (Figure 1)

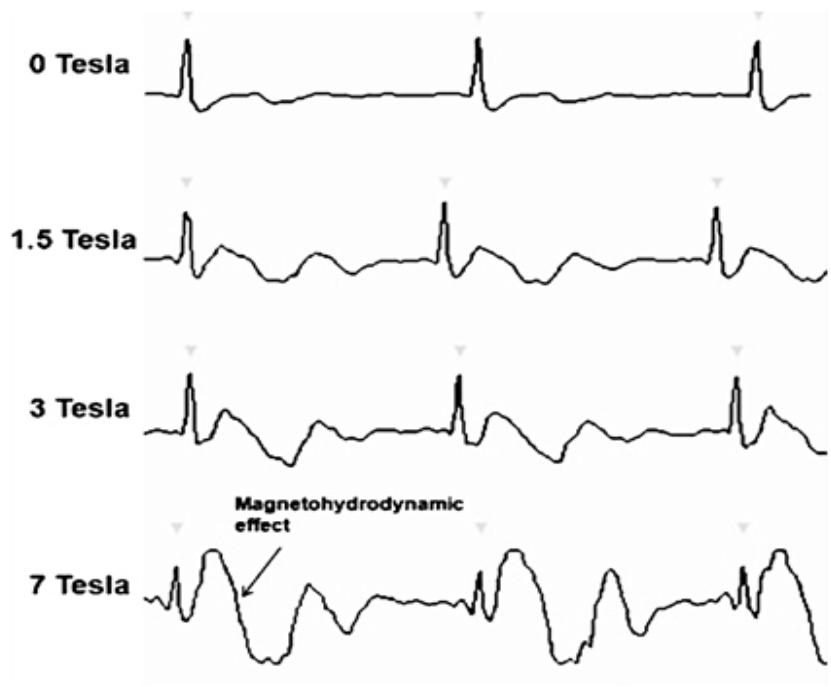

Figure 1. ECG traces at varying magnetic fields.
Source: Adapted from [2]

1.2.3 Challenges with Respiratory Motion Synchronization

Breath-holding is commonly used to eliminate respiratory motion, and its successful implementation can be very patient-dependent. To generate diagnostic quality images, patients are instructed to hold their breath during the acquisition. In general, multiple breath-holds of 5-20 second duration are required during the entire MRI scan that may take close to an hour to complete. This technique, however, can be unreliable because many patients are unable to hold their breath for the required time during scanning. Respiratory bellows can be used to track

respiratory motion but are not commonly used because they offer limited reliability. Navigator echoes are widely used for respiratory motion tracking. The signal generated by navigator echoes is used to limit the MRI acquisition to a specific phase of respiration. However, its setup requires additional time and expertise, and it is not compatible with many cardiac MRI sequences, for example, steady-state free precession sequence.

1.3 Proposed Solution for Cardiac MRI Challenges

The several limitations discussed in Section 1.2 highlight the need for a new and robust form of cardiac and respiration motion signal detection. A more efficient approach would entail tracking the respiratory and cardiac motion signals simultaneously regardless of the field strength.
Two relatively new techniques have been proposed and studied to track physiological motions. The first approach, termed as self-gating, offers a viable alternative to ECG and navigator echoes. This technique relies on MRI data to extract the cardiac and respiratory motion. Although recent studies highlight the potential of self-gating to extract physiological motions reliably [3, 4], this technique requires sampling patterns that periodically pass through the center of the k-space, which can lower the acquisition efficiency and demand pulse sequence modification. Another emerging approach called PT, is based on detecting the mechanical activity of the organs in the thoracic cavity. PT can simultaneously track cardiac and respiratory motion, and it does not require modification to the pulse sequence.

Chapter 2. Pilot Tone Cardiac Signal Extraction

2.1 Introduction to Pilot Tone

PT is an emerging technology in the field of cardiac MRI that can be used for tracking the mechanical activity of the organs in the thoracic cavity [5, 6]. PT utilizes a local external RF transmitter that is placed on or close to the thoracic cavity while the subject or patient is scanned using the MRI. The simple setup is illustrated in Figure 2. The signal from this transmitter is modulated by the physiological motions and, thereby, provides real-time motion tracking for the respiratory and cardiac motions. The resulting modulated signal is picked up by the MR receiver coils placed around the thoracic cavity. The large bandwidth of MR receivers allows for the PT frequency to be selected outside the imaging bandwidth. The non-overlapping frequencies of PT and MRI ensure that PT can be separated from the MRI data.

Additionally, PT is low-cost and can be integrated with any MRI application without additional setup time or modification to the pulse sequence [2]. This makes PT an attractive choice for physiological motion compensation and tracking when compared with the standard MRI setup described in Section 1.2. Furthermore, the quality of PT is not expected to be adversely affected by the magnetic field. Therefore, PT provides an efficient alternative that can circumvent the limitations present in ECG, respiratory bellows, navigator echoes, and breath-holding.

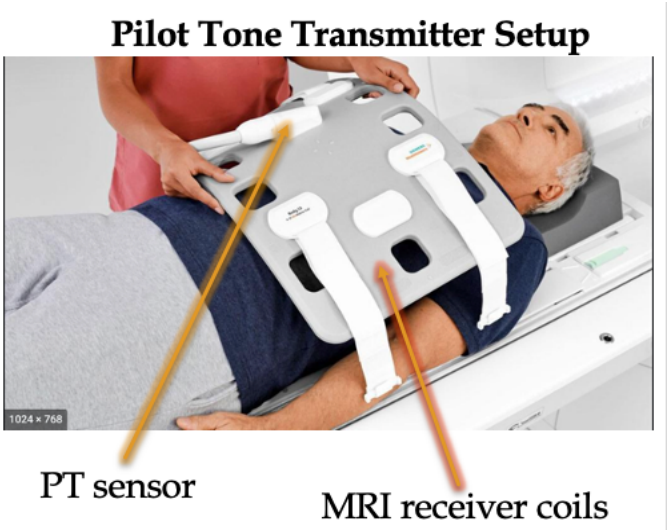

Figure 2. PT transmitter setup for subject prior to an MRI scan.

Source: Adapted from [7]

2.2 PT Channels and Signal Extraction

From the signal measured at the MRI receiver coils, also called channels, the PT raw data is easily separated from the MRI signal due to the significant difference in their frequencies. To highlight the encoding capability of PT, it has been shown in [6] and [8] that there is detectable cardiac information stored in PT raw data that can be extracted for motion synchronization in cardiac MRI. Depending on the position of each channel with respect to the heart, the cardiac motion signal is encoded in all channels but to varying degrees. An example of a complex-valued PT channel is displayed in Figure 3. This data was collected over a span of roughly 300 seconds from a healthy subject. Both respiratory (slow cycles) and cardiac (fast cycles) signals are visible in the raw data.

In a recent study conducted by Bacher et al., it was observed that the cardiac motion was not localized to a single channel but was spread across all the PT channels [2]. Therefore, generally, all PT channels are jointly processed to extract the cardiac motion signal.

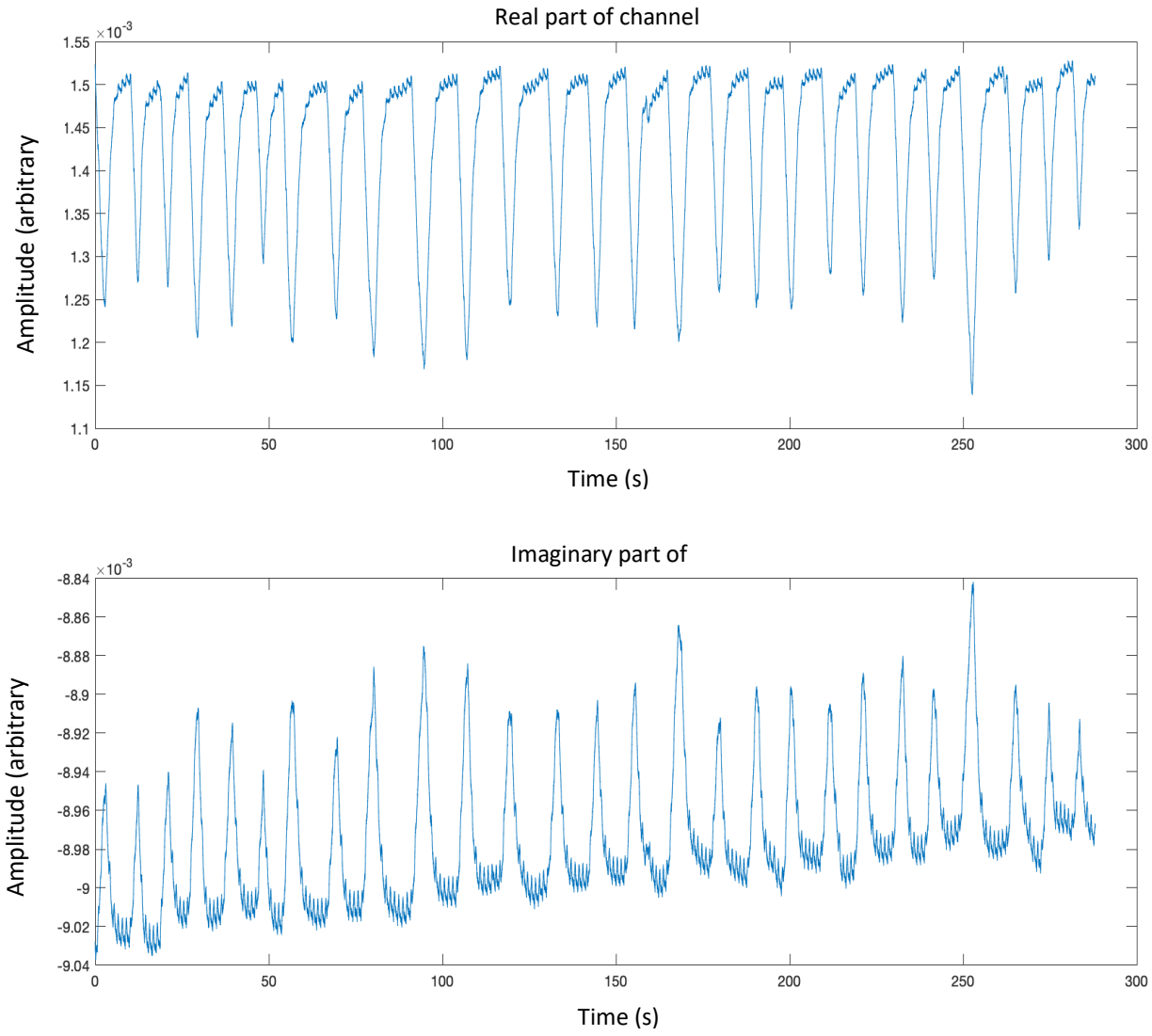

Figure 3. One channel from a total of 24 channels of healthy subject's PT raw data.

2.3 Previous Research and Findings in the Area of PT

The signal received at each channel is a linear, unknown mixture of the physiological motions. Separating these sources, without prior knowledge of the source's characteristics, can be posed as a blind source separation problem [10]. The recent work conducted by Bacher et al. describes an algorithm to extract the cardiac signal from the raw multi-channel PT data [2]. The algorithm is based on the combination of principal component analysis (PCA), independent component analysis (ICA), and bandpass filtering. PCA is primarily used to reduce the number of channels, and ICA is then employed to separate the respiratory and cardiac motion signals. More recently, Chen et al. also used a similar algorithm to successfully extract the cardiac and respiratory signals from patients' PT data [9].

The strong agreement between the PT-derived cardiac triggers and ECG triggers in the studies by Bacher et al. and Chen et al. points to the potential of replacing ECG with PT in the field of cardiac MRI. However, there are no studies that compare different algorithms for extracting the cardiac and respiratory signals from the raw PT data. Moreover, it is unclear whether this combination of PCA and ICA is robust to a low signal-to-noise ratio or the presence of electromagnetic interference.

2.4 Challenges with PT

Typically, the PT data is free from artifacts and has an adequate signal-to-noise ratio for cardiac signal extraction. However, due to long scan times, it not uncommon to see patient movements

and noise from surrounding electronics interfere with the PT signal. Also, the patient's movement, a faulty receiver coil, or noise from electronics may not contaminate all PT channels equally; the contaminated PT data may have channels with varying signal quality. The inconsistencies in signal quality can make the extraction of the cardiac signal more challenging. Figure 4 and Figure 5 show a clean dataset and a dataset with a few corrupt channels, respectively. These two figures correspond to the datasets from 2 healthy subjects (A1 and A2) scanned for approximately 300 seconds on a 1.5 Tesla MRI scanner with the PT transmitter setup. Only five complex-valued channels (from a total of 24) are illustrated for visual comparison. It is evident that the data from A2 has more artifacts, perhaps, due to bulk motion. The periodic cardiac and respiratory motion signals are clearly visible in data from A1 (see Figure 4); however, these physiological motions are overwhelmed by strong intermittent interference in data from A2 (see Figure 5). By efficiently discarding the few corrupt channels, the encoded cardiac signal can still be recovered. Discarding these corrupt channels manually is feasible but not practical. Therefore, there is an unmet need to develop an automatic approach to discard corrupt channels from the PT data.

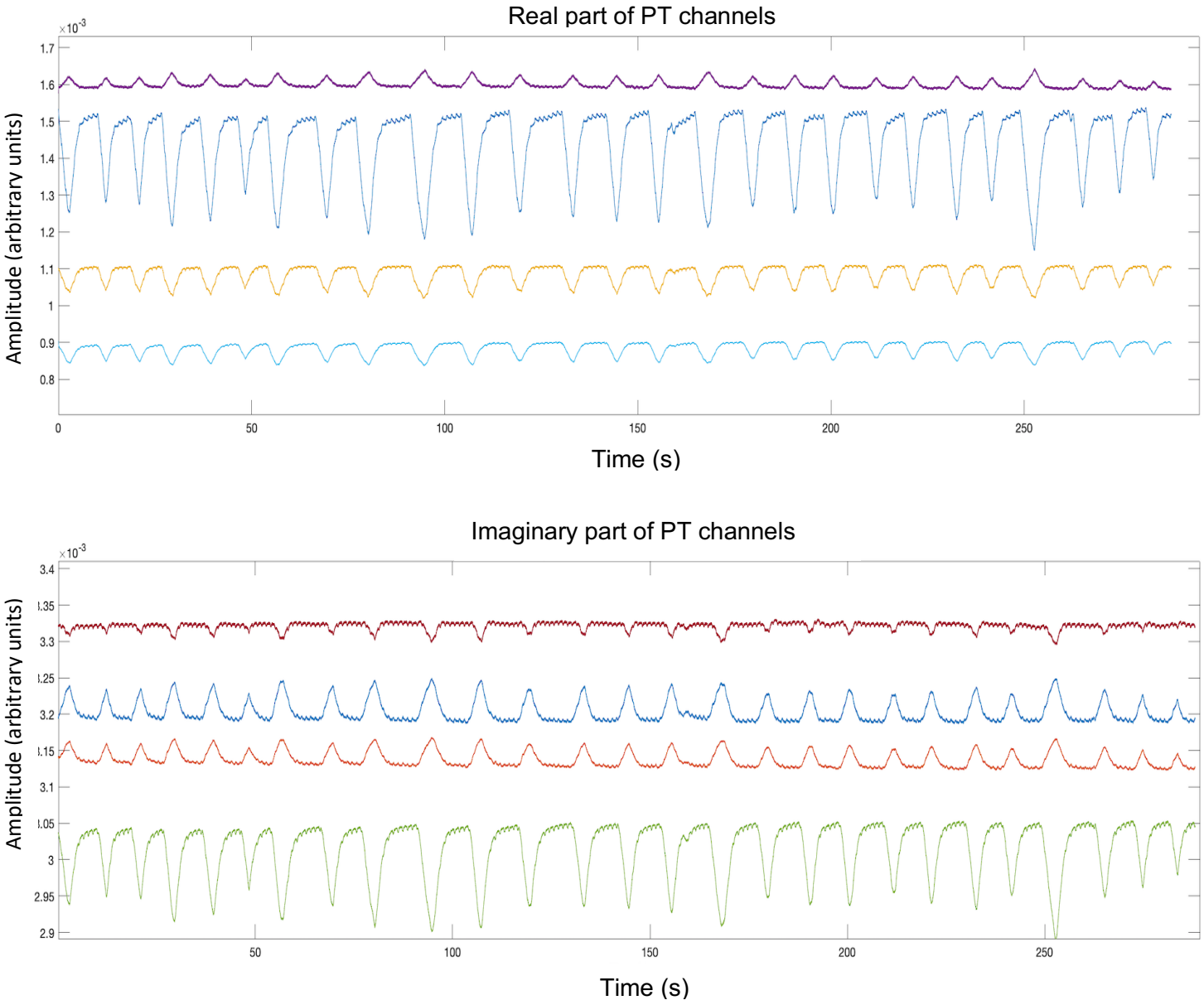

Figure 4. Dataset with clean PT channels. Five channels from a total of 24 channels of the healthy subject A1.

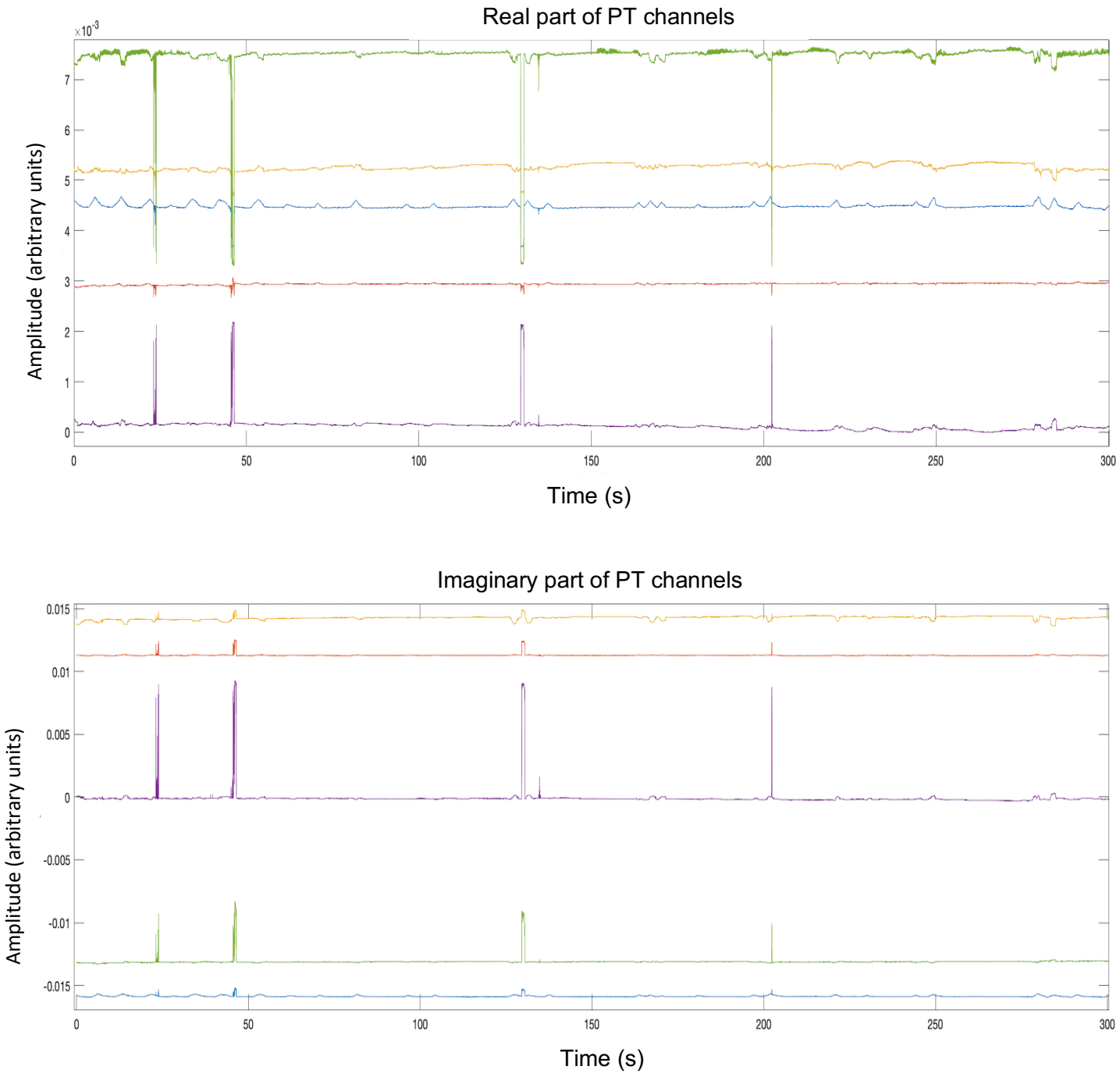

Figure 5. Dataset with a few corrupt channels. Five channels from a total of 24 channels of the healthy subject A2.

2.5 Possible Solution to PT Challenges

To improve the extraction of cardiac signal from partially corrupt raw PT data, we propose an automatic method to suppress interference. For cardiac MRI, the concept of channel pruning has been explored previously for self-gating. Recently, a study by Feng et al. describes a spectral analysis-based channel pruning approach to facilitate cardiac signal extraction [11]. Although a similar procedure can be applied to PT, it does not take into account the vastly different signal-to-noise ratios or artifact-levels of PT channels into account. In the following sections, we describe a processing pipeline to extract the cardiac signal from raw PT data. In addition, we propose a new channel pruning operation to improve its performance further.

Chapter 3. Cardiac Signal Extraction Pipeline

3.1 Terminology

N – Number of PT samples collected

N_i – Number of PCA channels

K – Number of raw PT channels

$P_0 \in \{\mathbb{C}^{N\times K}\}$ – Multi-channel complex-valued raw PT data

$P_0' \{\in \mathbb{R}^{N\times 2K}\}$ – Real-valued PT data constructed by concatenation of real and imaginary parts

$P_i \{\in \mathbb{R}^{N\times N_i}\}$ – Reduced PT data after the PCA processing

$P_f \{\in \mathbb{R}^{N\times 1}\}$ – Cardiac signal (one channel cardiac signal after the ICA processing)

$C \{\in \mathbb{R}^{N\times 1}\}$– Filtered cardiac signal

C_T – PT-derived cardiac trigger locations

E_T – ECG-derived cardiac trigger locations

3.2 Existing Pipeline for Cardiac Signal Extraction from PT Data

The PT-derived cardiac triggers can be extracted using the pipeline recently proposed in [9]. The pipeline is shown in Figure 6 and is described below:

- The complex-valued multi-channel raw PT data (P_0) is converted to real-valued multi-channel PT data (P_0') by concatenating the real and imaginary parts of P_0.

- For the purpose of dimensionality reduction, P_0' is processed using principal component analysis (PCA) to reduce the number of channels to N_i. These N_i channels correspond to

the set of the N_i largest singular values. The resulting data P_i has lower dimensions but preserves the salient features of P_0.

- Independent component analysis (ICA) is then performed on P_i to separate the physiological motions. To increase robustness and reliability, the ICA is repeatedly performed five times on P_i to get five possible choices for the cardiac signal. The energy of the five signals is compared in frequency domain and the signal with the highest peak in the bandwidth 0.5 Hz – 3 Hz range is selected as the cardiac signal (P_f).

- For noise suppression, P_f is filtered with a bandpass filter with a bandwidth 0.5 Hz – 3 Hz, to yield the filtered cardiac signal (C). Sign determination is applied using the approach in [12] to ensure that the cardiac signal has the correct polarity.

- Cardiac signal triggers (C_T) are extracted by taking the first order derivative of C and performing peak selection on the negative peaks.

- ECG triggers (E_T) collected during the MRI scan and C_T are compared and analyzed.

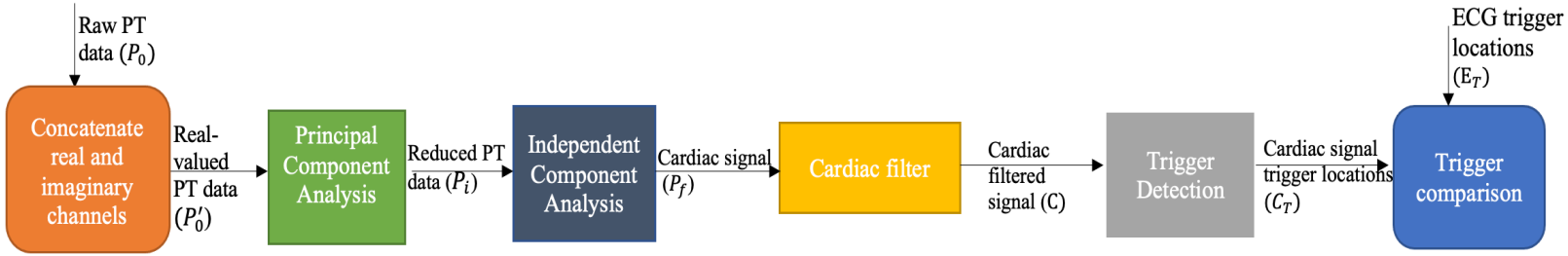

Figure 6. Existing pipeline for PT cardiac signal extraction and trigger comparison. ECG-derived cardiac triggers are used as reference.

3.3 Pipeline Challenges and Need for Optimization

The existing pipeline was used to test subjects A1 and A2 that were discussed previously in Section 2.4. The raw PT data and the resulting cardiac signals are shown in Figures 7, 8, 9, and 10. When comparing the raw PT data from subjects A1 and A2 (Figures 7 and 9), it is clear that some of the channels in the data from A2 were corrupted, whereas the data from A1 was quite clean. The effect of using these channels in the existing pipeline can be observed more clearly in Figures 8 and 10. The cardiac signal from A1 is clean and semi-periodic; however, the cardiac signal from A2 is not accurate. In summary, the existing pipeline performs well for clean or relatively clean datasets, but the pipeline is not robust enough to handle corrupt channels.

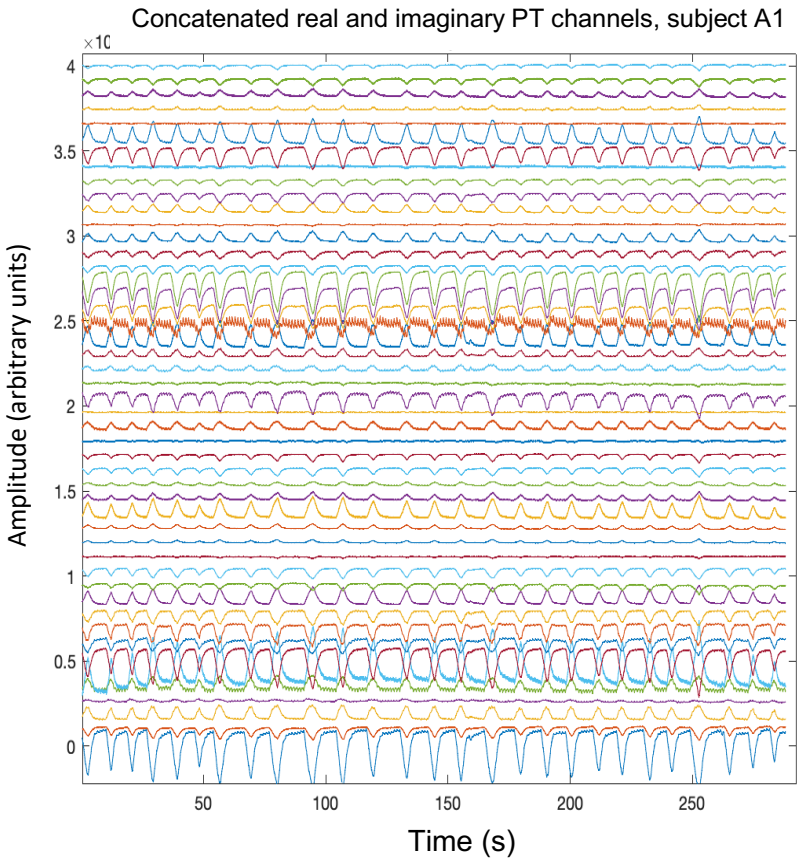

Figure 7. Concatenated real and imaginary channels of PT, subject A1

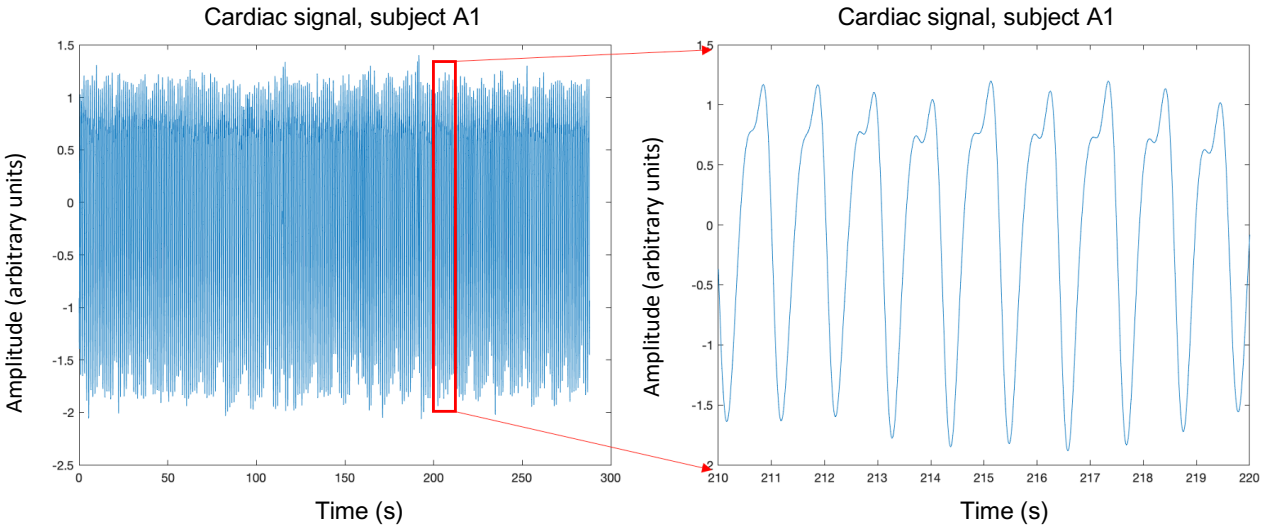

Figure 8. Extracted PT cardiac signal, subject A1.

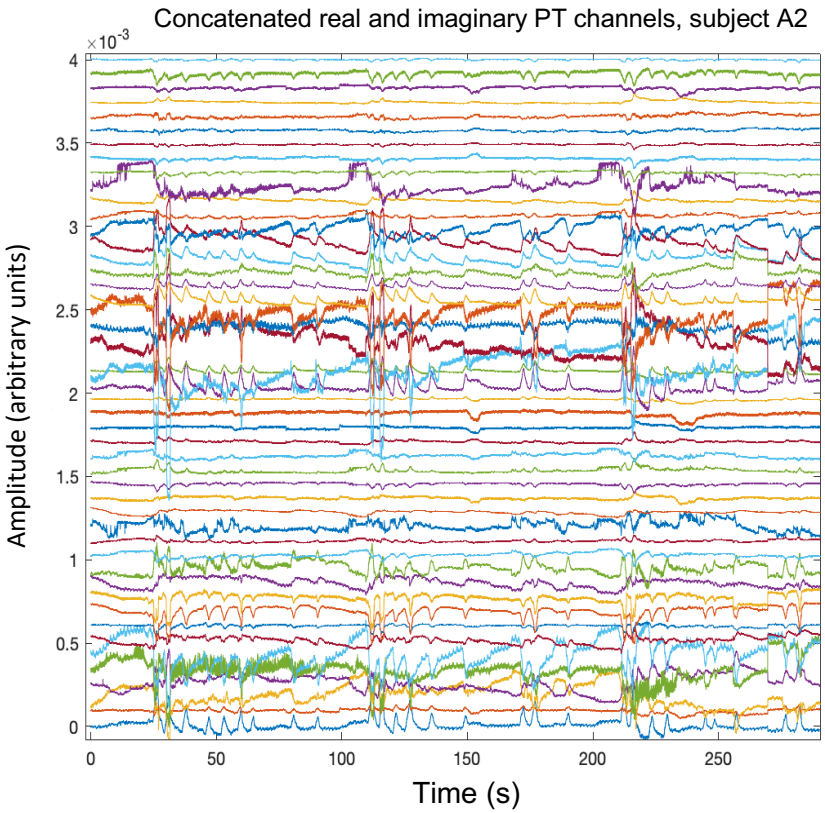

Figure 9. Concatenated real and imaginary channels of PT, subject A2.

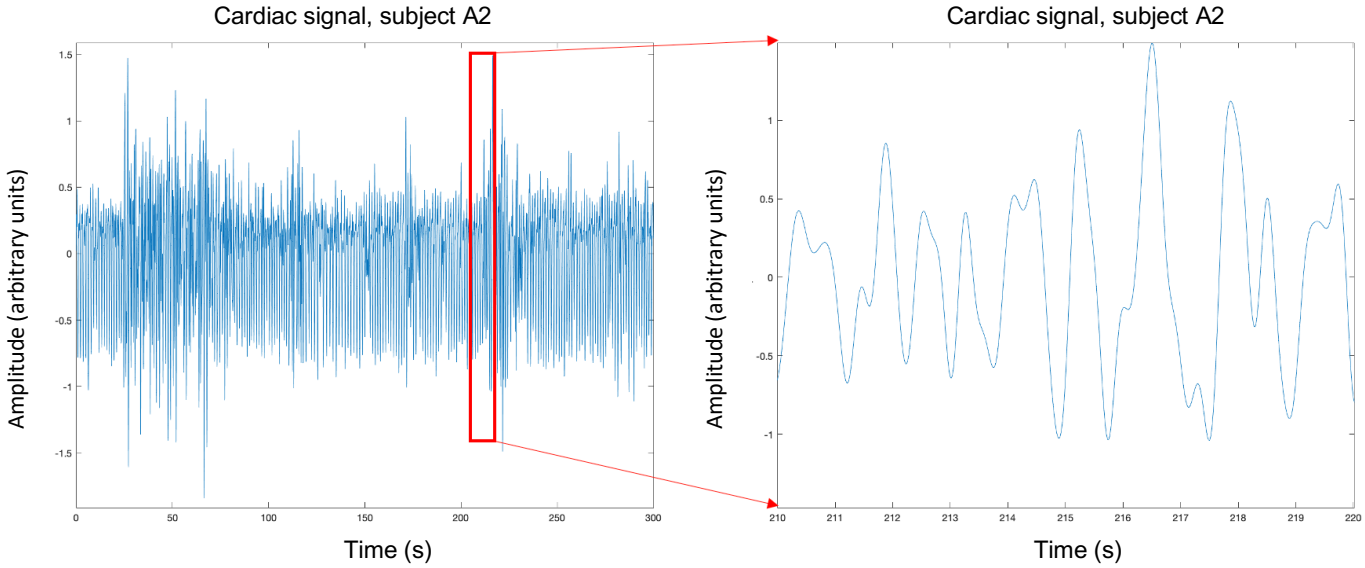

Figure 10. Extracted PT cardiac signal, subject A2.

3.4 Optimization of the Existing Pipeline

3.4.1 ROVir Concept

Beamforming is a strategy used in the field of sensor array processing to maximize the signal of interest and minimize the interference signal. A recently proposed approach, region-optimized virtual coils (ROVir), introduced by Kim D. et al., illustrates an application of beamforming concepts for MRI coil compression [13]. In MRI, the field-of-view (FOV) is typically larger than the region-of-interest (ROI). Also, the MRI receiver coils are physically displaced from one another and thus modulate the FOV differently. ROVir seeks to linearly combine physical channels (receiver coils) to create virtual channels, called ROVir coils. These ROVir coils are sorted such that the ratio of the signal energy inside the ROI to outside the ROI is maximum in the first channel and minimum in the last channel. This sorting strategy allows a natural way to discard some of the latter coils that have small relative energy inside the ROI. Subsequently, a smaller number of compressed ROVir coils can then be used for further processing. Compared to the original coils, ROVir coils may improve the image quality by discarding signals outside the ROI and facilitate faster image processing [13]. The concept of ROVir is depicted in Figure 11.

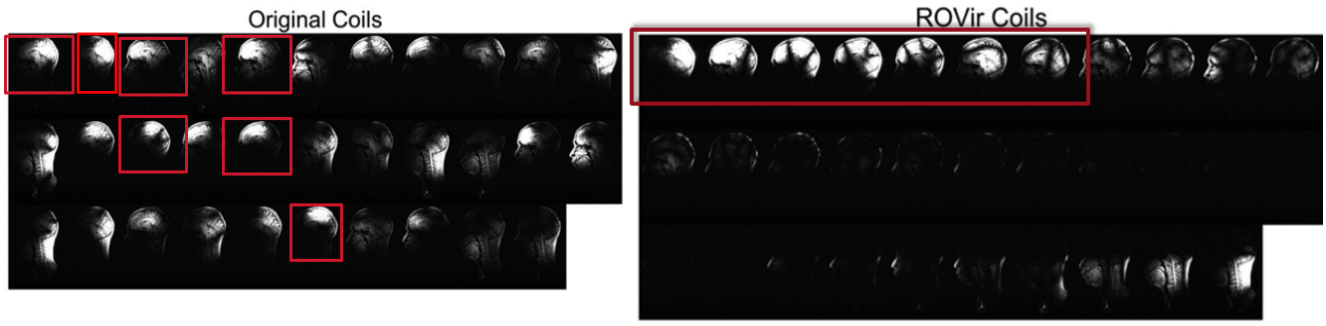

Figure 11. Illustration of original MRI coils and ROVir coils.

Source: Adapted from [11].

3.5 BOSyn channels: bandwidth-optimized synthetic channels

3.5.1 Terminology for BOSyn

Some of the terminologies used below have been described in Section 3.1.

H – Hermitian or conjugate transpose

N_c – Number of raw PT channels

N_s – Number of synthetic channels after BOSyn processing

N_R – Number of frequency domain samples in ROI

N_T – Number of frequency domain samples in INR

F $\{\in \mathbb{C}^{N \times N_c}\}$ – Fast Fourier Transform (FFT) matrix

F_{ROI} $\{\in \mathbb{C}^{N_R \times N_c}\}$ – ROI selected in frequency domain

F_{INR} $\{\in \mathbb{C}^{N_T \times N_c}\}$ – Interference region (INR) selected in frequency domain

$\boldsymbol{V}$ $\{\in \mathbb{C}^{N_c \times N_c}\}$ – Inter-channel frequency domain correlation matrix of PT data within ROI

$\boldsymbol{U}$ $\{\in \mathbb{C}^{N_c \times N_c}\}$ – Inter-channel frequency domain correlation matrix of PT data in INR

SIR $\{\in \mathbb{R}^{1 \times N_c}\}$ – Signal-to-Interference Ratio

$\boldsymbol{w}$ $\{\in \mathbb{C}^{N_c \times N_c}\}$ – Columns of this matrix are used as weights to create BOSyn channels

$\lambda\{\in \mathbb{R}^{1 \times N_c}\}$ – Eigen values corresponding to the eigen vectors (columns) in $\boldsymbol{w}$

3.5.2 Optimized Pipeline Setup

In this work, we propose a method to automatically prune PT channels. This technique is adapted from the ROVir approach to create BOSyn channels. These BOSyn channels can be used as inputs to the existing pipeline in place of the raw PT channels. The strategy for designing BOSyn channels is illustrated in Figure 12, and its main steps are described below.

1. With the raw PT data (P_0) as input, a Fast Fourier Transform (FFT) is performed along the time dimension to create a new matrix, F.
2. F is then decomposed into two non-overlapping regions F_{ROI} and F_{INR}. F_{ROI} is selected to be -4 Hz to 4 Hz region to include the cardiac signal and its harmonics. F_{INR} is selected to be all frequencies below -6 Hz and above 6 Hz.
3. Hermitian symmetric matrices $\boldsymbol{V}$ and $\boldsymbol{U}$ are computed using Equations 1 and 2, respectively.

$$\boldsymbol{V} = F_{ROI}^{H} F_{ROI}$$

Equation 1: Inter-channel frequency domain correlation matrix of PT data within ROI

$$\boldsymbol{U} = F_{INR}^{H} F_{INR}$$

Equation 2: Inter-channel frequency domain correlation matrix of PT data in INR

4. $\boldsymbol{w}$ and λ are calculated via a generalized eigenvalue decomposition of $\boldsymbol{U}$ and $\boldsymbol{V}$ (see Equation 3). Then, λ and $\boldsymbol{w}$ are sorted in descending order based on λ. The SIR is computed using $\boldsymbol{w}, \boldsymbol{U},$ and $\boldsymbol{V}$(see Equation 4). As the columns of $\boldsymbol{w}$ are already sorted based on λ, it is observed that the first column $\boldsymbol{w}_1$, maximizes the SIR criterion.

$$\boldsymbol{V}\boldsymbol{w}_k = \lambda_k \boldsymbol{U}\boldsymbol{w}_k$$

$$(where\ k \in 1, \dots, N_c)$$

Equation 3: Generalized Eigenvalue decomposition

5. From a total of N_c columns of $\boldsymbol{w}$, only the first N_s columns are used for performing a linear combination of P_0 to yield the BOSyn channels.

$$\boldsymbol{SIR}(\boldsymbol{w}_k) = \frac{\boldsymbol{w}_k^{\boldsymbol{H}} \boldsymbol{V} \boldsymbol{w}_k}{\boldsymbol{w}_k^{\boldsymbol{H}} \boldsymbol{U} \boldsymbol{w}_k}$$

$$(where\ k \in 1, \dots, N_c)$$

Equation 4: Signal-to-Interference Ratio

For visual illustrations, raw PT data from subject A2 was used for comparing the BOSyn channels and raw PT channels; see Figures 13 and 14. As expected, the energy in the first N_s BOSyn channels (12 channels for subject A2) is localized to -4 Hz to 4 Hz range. Compared to the PT channels in Figure 10, BOSyn channels in Figure 15 have a diminished level of interference. For trigger detection and subsequent analysis, these BOSyn coils are fed into the existing pipeline as inputs (see Figure 6).

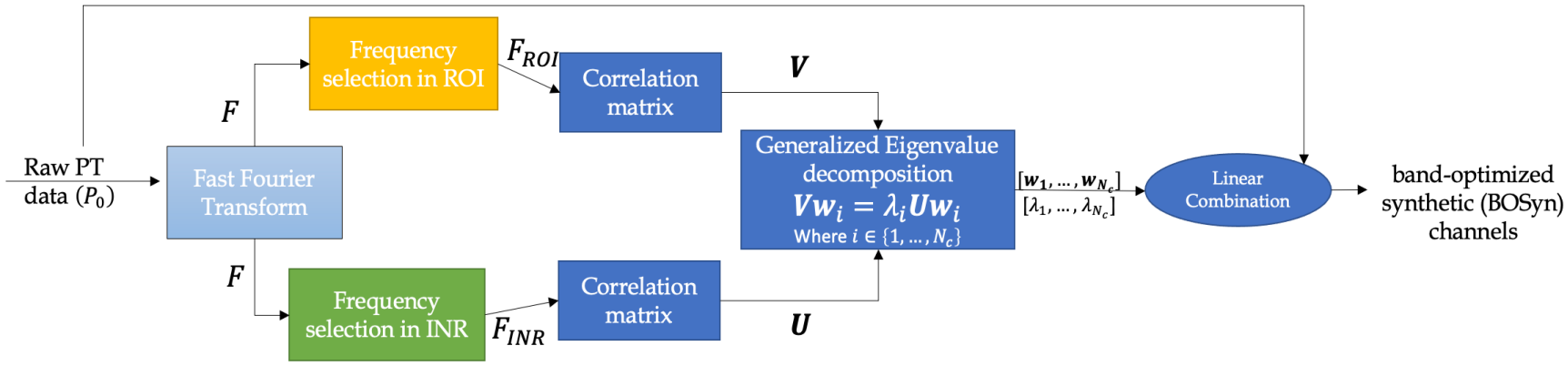

Figure 12. BOSyn channel creation methodology for raw PT channels.

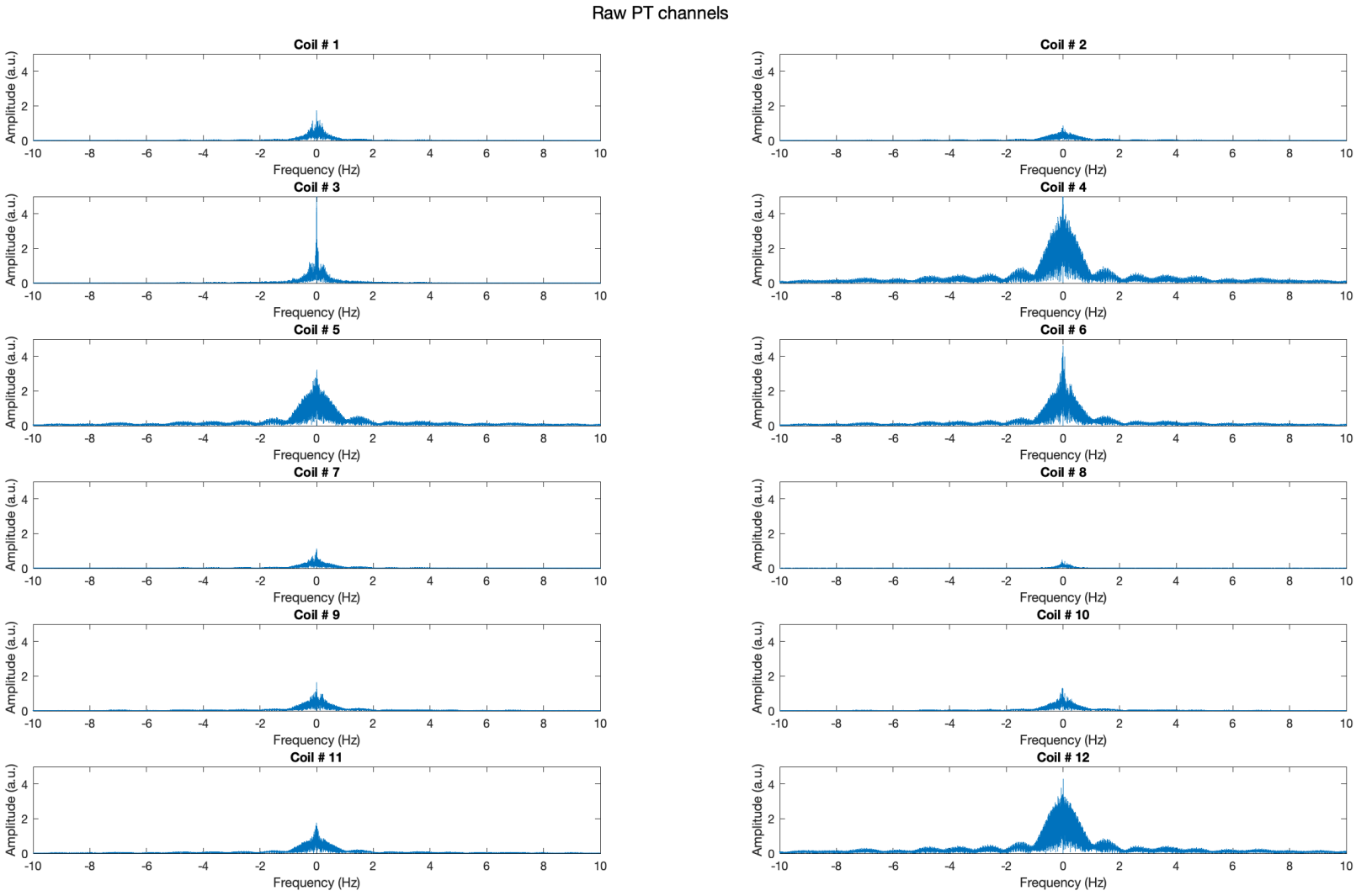

Figure 13. Absolute values of the raw PT channels in Fourier domain.

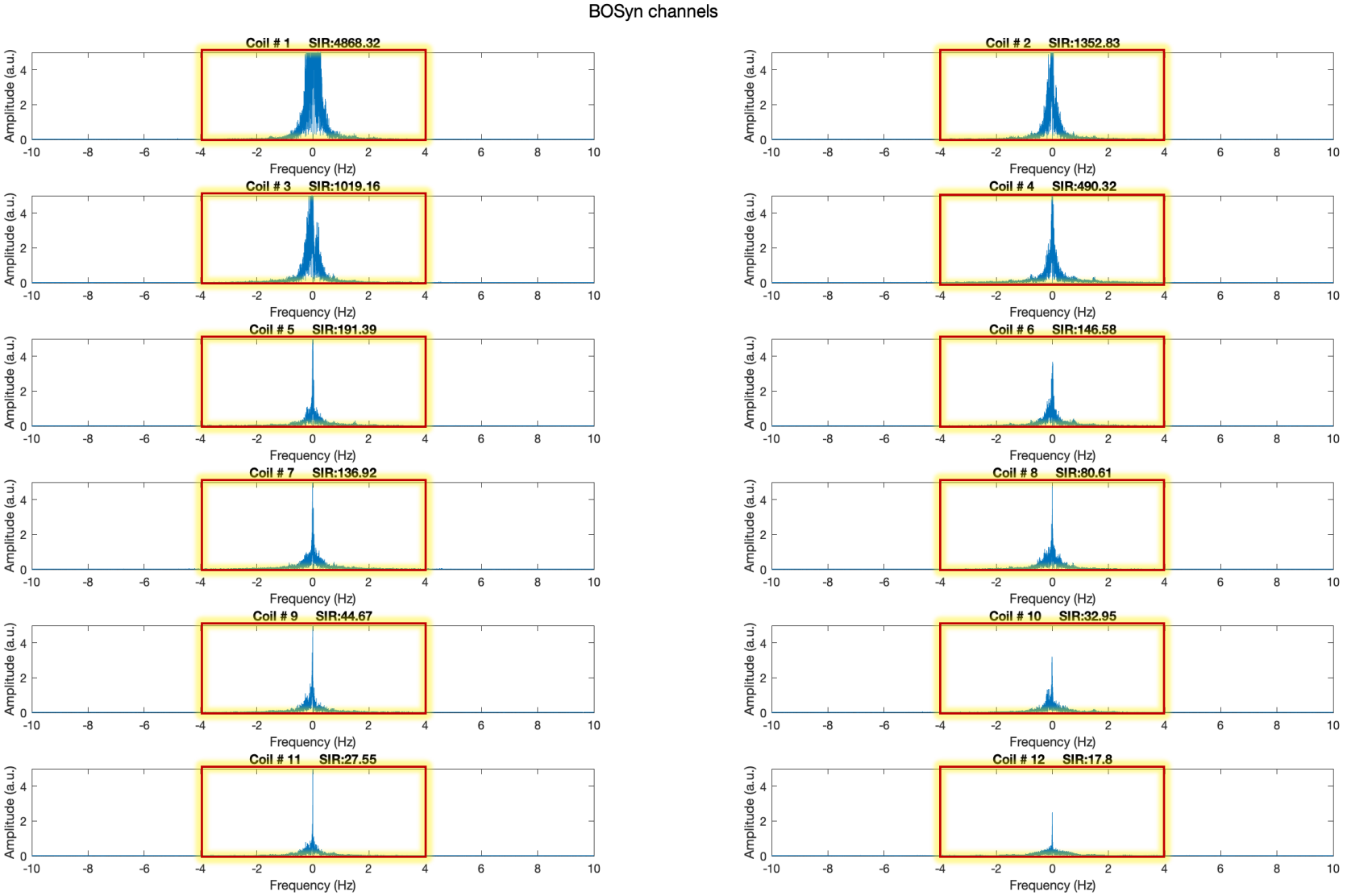

Figure 14. Absolute values of the BOSyn channels in Fourier domain.

The boxes in red highlight the region-of-interest (ROI).

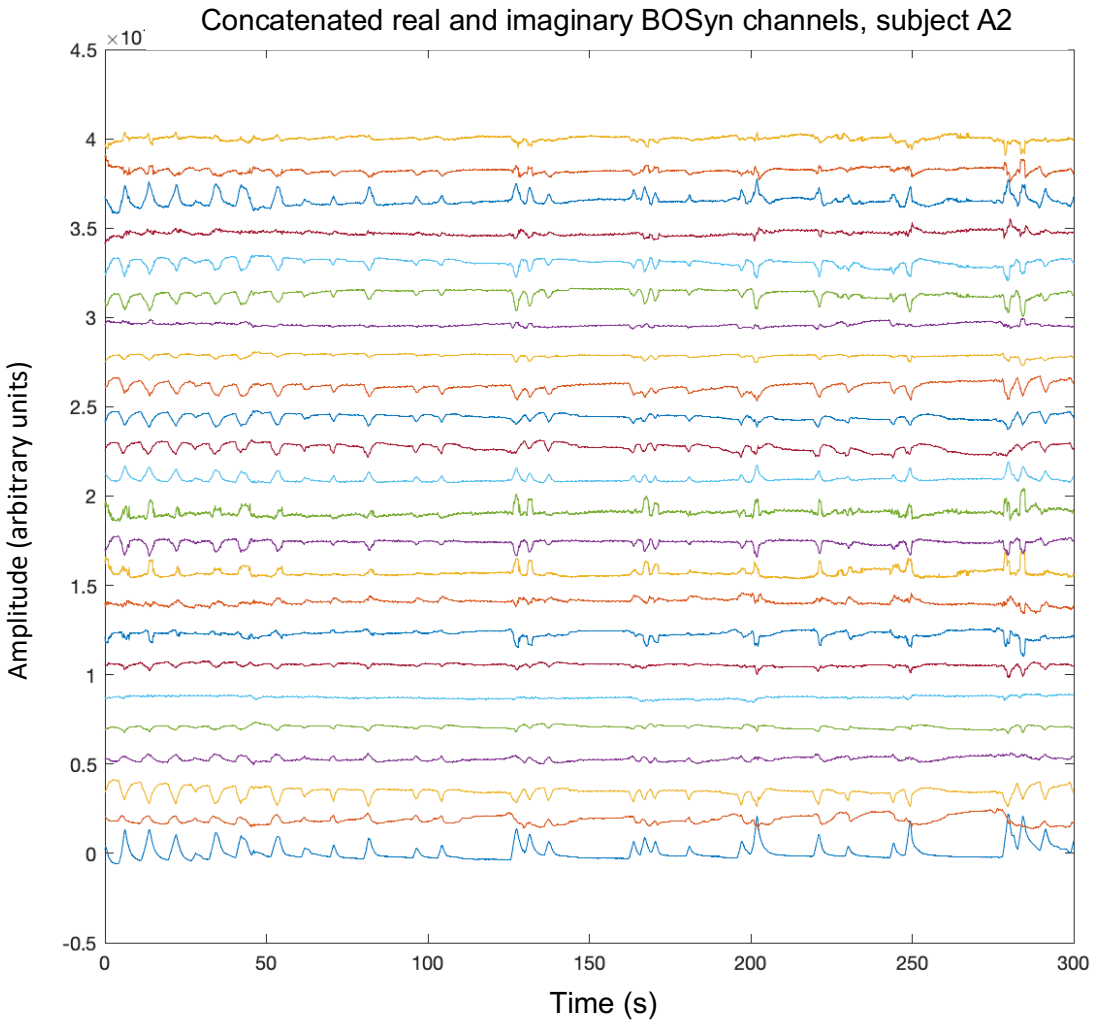

Figure 15. Real and imaginary parts of the first 12 BOSyn channels, subject A2. Compared to Figure 10, an improvement in signal quality is evident.

Chapter 4. Methodology

4.1 Experimental Validation

For validation, 14 healthy subjects were scanned on a 1.5 Tesla MRI scanner with the PT setup described in Figure 2. Most subjects were scanned for approximately 300 seconds and a few were scanned for approximately 600 seconds. For all 14 subjects both PT data and ECG data were acquired simultaneously. The pulse sequence used for all 14 subjects was Gradient Echo (GRE) based 4-D flow sequence. The sampling rate for ECG signal was 2.5 milliseconds (for all 14 datasets). The sampling rate for the PT signal varied among different subjects but were all within the range of 4.2 milliseconds and 4.8 milliseconds; see Table 1.

All 14 datasets were analyzed using the existing pipeline and the optimized pipeline (BOSyn channels + existing pipeline).

4.2 Terminology used for comparing PT derived cardiac triggers and ECG triggers

Some of the terminologies used below were explained in Sections 3.1 and 3.5.1.

False Positive (FP) – Absence of an E_T trigger in the range of ± 0.4 seconds of a given C_T trigger.

False Negative (FN) – Absence of a C_T trigger in the range of ± 0.4 seconds of a given E_T trigger.

Paired / Matched – A C_T trigger is present in the range of ± 0.4 seconds of a given E_T trigger.

After the C_T and E_T triggers are extracted using peak-picking, a small preliminary search is done for the purpose of trigger alignment. Since ECG and PT are sensitive to the electrical and

mechanical activities, respectively, a slight offset is routinely observed between the locations of the C_T and E_T triggers. To correct for this offset, for each ECG trigger, the distance of the nearest PT trigger is computed and stored. Then a simple offset correction is carried out by subtracting the median value of all the pairwise distances from C_T . Once the C_T and E_T triggers are aligned they are binned into FN, FP, and paired triggers. The standard deviations of the pairwise distances between the matched C_T and E_T triggers are also computed. (See Table 1)

Figure 16 provides a visual interpretation of how C_T and E_T are paired after the alignment process. When a C_T trigger is within 0.4 seconds on either side of an E_T trigger, then it is concluded that those 2 triggers arise from the same heartbeat and thus match. In addition, the locations of FP and FN triggers are highlighted along with the region for matched or paired C_T and E_T triggers.

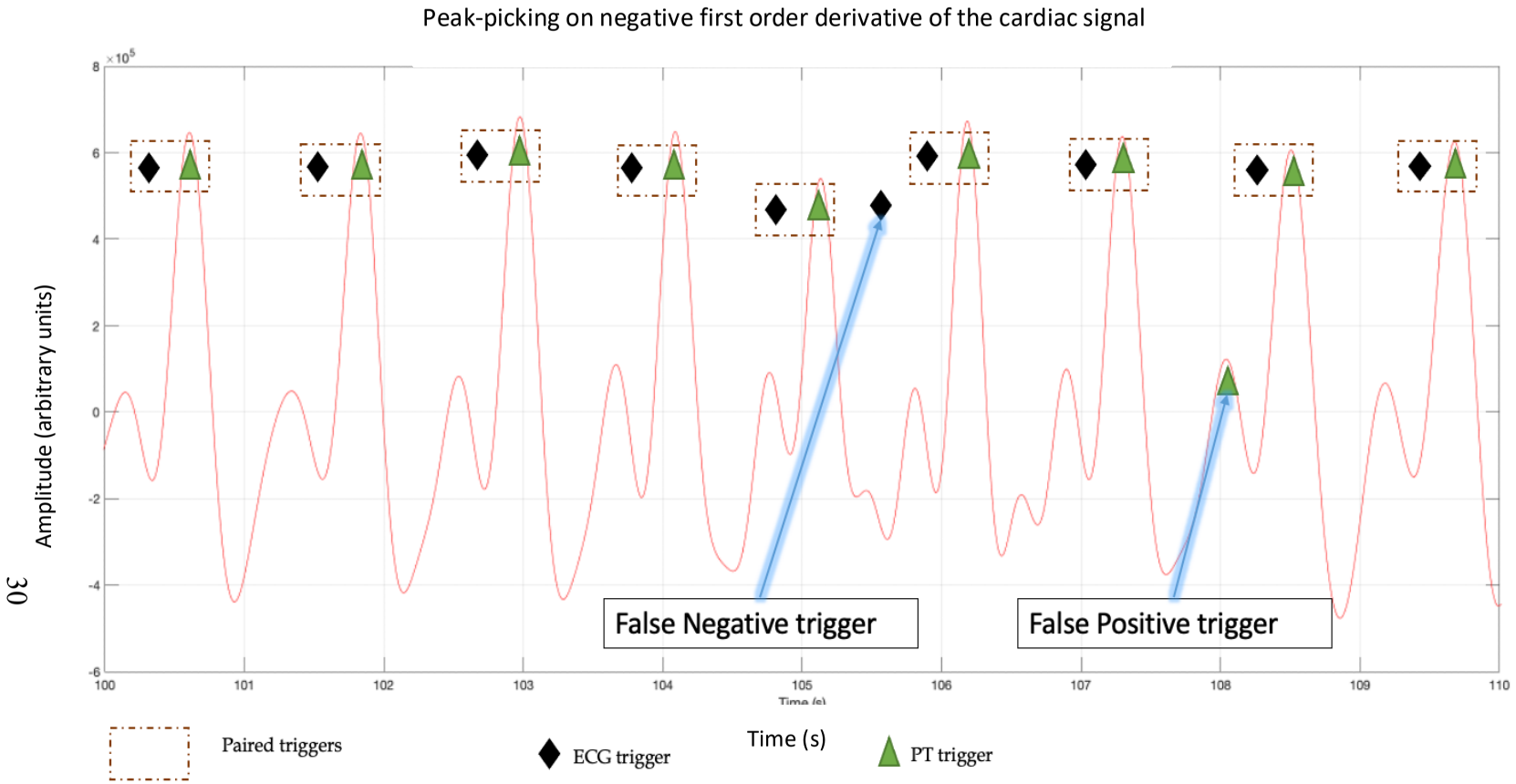

Figure 16. Trigger comparison between PT triggers and ECG triggers with ECG triggers as reference. PT-derived cardiac signal over a span of 10 seconds is shown.

4.3 Results

The results highlighted in Table 4.1 can be interpreted as follows:

- Nine out of the 14 datasets resulted in a comparable performance between the existing pipeline and the optimized pipeline. These datasets were visually clean, and the observed results were just as expected. The difference of 2-3 triggers among these datasets is well within the 5% error threshold that was hypothesized in this study.

- Four out of the 15 datasets resulted in significantly better performance for the optimized pipeline compared to the existing pipeline. The datasets 5 and 8 had only a few corrupt channels in the raw PT data, and the optimized pipeline was able to eliminate most of the FP and FN triggers. However, datasets 7 and 9 had a large number of severely corrupt channels. For these two datasets, the optimized pipeline provided an improvement over the existing pipeline but was unable to remove some of the FP and FN triggers. It is unlikely that the PT data would be corrupted to this degree. The primary reason for including these datasets in the study was to test the robustness of the optimized pipeline. Also, datasets 7 and 9 may benefit from additional optimization to the signal extraction process.

- Dataset 12 was the only one where the optimized pipeline performed slightly poorly compared to the existing pipeline. In particular, the number of FP and FN triggers increased from 0 and 1 to 4 and 15, respectively. Since the cardiac signal extracted from the optimized pipeline was visually cleaner than the one extracted using the existing

pipeline (see Figure 17), it was not clear why the optimized pipeline had higher instances of FP and FN triggers. We conjecture that a possible area for failure for dataset 12 could be the error in trigger alignment between the PT-derived triggers and the ECG-derived triggers. The trigger alignment step explained in Section 4.2 is crucial in the detection of matched, FP, and FN triggers. A misalignment by a single trigger can lead to a significant disagreement between C_T and E_T. In our future work, we plan to revisit the alignment strategy.

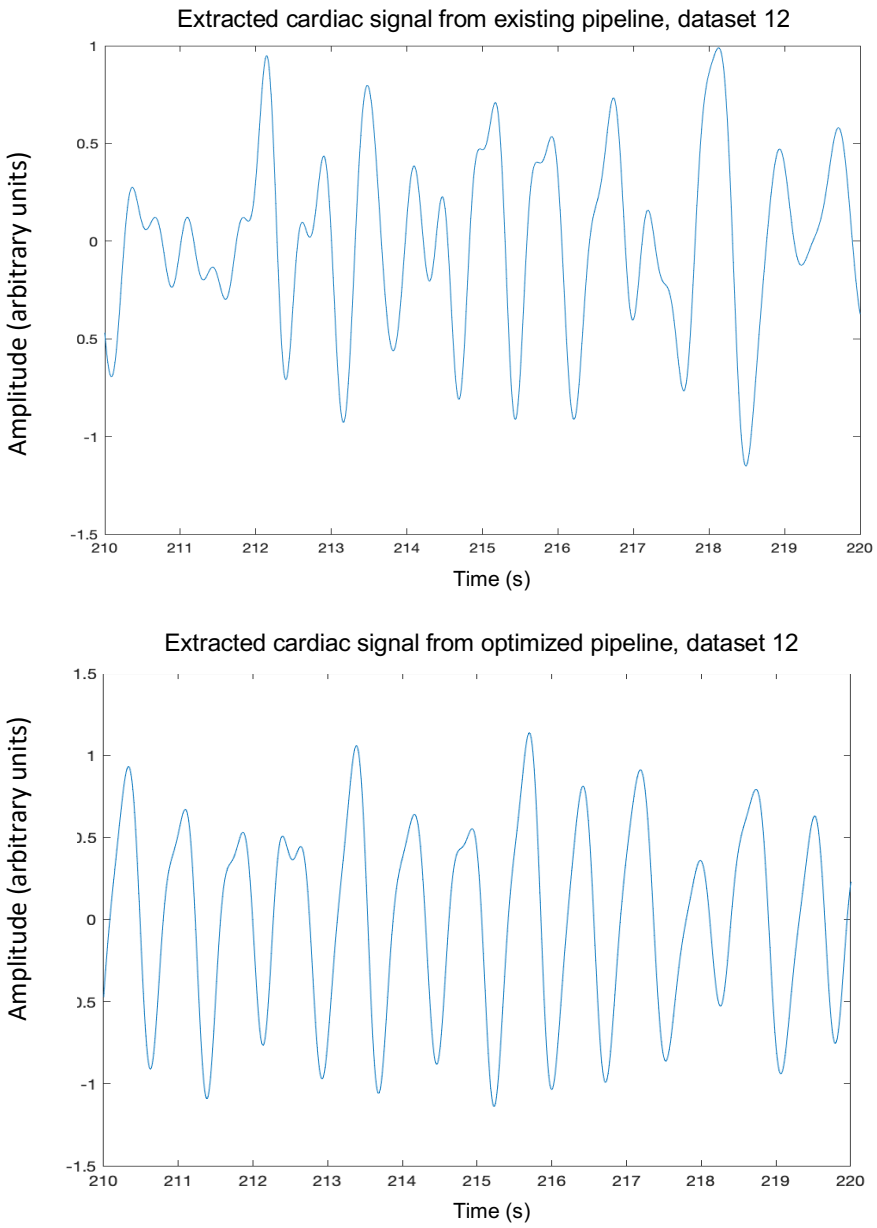

Figure 17. A visual depiction of the extracted cardiac signal from the existing and optimized cardiac pipeline.

The signals over the span of 10 seconds are shown for comparison.

Chapter 5: Conclusions and Future Work

5.1 Summary and Conclusion

Extraction of the cardiac and respiratory signal is essential for generating diagnostic quality images in cardiac MRI. PT-based physiological motion extraction is an emerging avenue, but it needs to be validated and optimized. This work presents a unique approach to compress the raw PT channels into synthetic channels which can help eliminate artifacts and interference. Based on the results from the study conducted on 14 subjects, we conclude that the presented optimized pipeline provides an improvement over the existing pipeline in terms of trigger extraction, accuracy and precision.

5.2 Future Work

In the future, we will validate this technique using data from patients. Note, patients with cardiac diseases often have arrhythmias and thus have more irregular cardiac signals. This will be important to evaluate the generalizability of the optimized pipeline. Moreover, we will further optimize the process of alignment between ECG-derived triggers and PT-derived triggers. The alignment might have contributed to some of the FP and FN triggers observed in Table 1. Finally, although we have exclusively focused on the cardiac signal extraction in this work, the proposed pipeline can benefit the extraction of the respiratory signal as well. This hypothesis will be tested and evaluated in future studies.

Table 1. Analysis of 14 datasets of scanned subjects.

Sampling Rate PT (seconds)	Dataset	Reference ECG Triggers	EXISTING PIPELINE				OPTIMIZED PIPELINE			
			PT Triggers	False Positive	False Negative	Std-Dev	PT Triggers	False Positive	False Negative	Std-Dev
0.00463	1	258	257	0	1	1.41E-04	257	0	1	4.40E-03
0.00465	2	243	243	0	0	9.79E-05	243	0	0	7.40E-04
0.00444	3	307	306	0	1	3.80E-03	308	1	0	3.10E-03
0.00424	4	26	26	0	1	4.07E-05	26	0	0	3.19E-04
0.00463	5	350	349	37	61	9.20E-03	351	3	2	2.50E-03
0.00469	6	624	626	1	1	7.28E-05	625	1	0	1.30E-03
0.00458	7	243	380	246	109	4.03E-02	248	99	95	4.62E-02
0.00469	8	355	335	5	25	3.70E-03	354	1	2	3.30E-03
0.00473	9	348	240	52	160	3.30E-02	346	4	8	5.50E-03
0.00473	10	545	545	0	0	7.38E-05	545	0	0	1.40E-03
0.00467	11	678	677	0	1	9.94E-05	678	3	3	3.90E-03
0.00473	12	395	394	0	1	8.50E-04	396	4	15	3.89E-02
0.00462	13	340	340	0	0	2.20E-03	340	0	0	2.20E-03
0.00473	14	480	481	1	1	2.74E-04	480	0	0	1.90E-03

OPTMIZED PIPELINE room for improvement by tuning	Tie (~2-3 triggers)	Superior performance	Inferior performance

Bibliography

[1] M. Zaitsev, J. Maclaren, and M. Herbst. Motion Artefacts in MRI: a Complex Problem with Many Partial Solutions. *J. Magn. Reson. Imag.*, 42(4):165–187, 2015. ISSN 2045-2322. doi: 10.1007/128.

[2] M. Bacher, "Cardiac Triggering Based on Locally Generated Pilot-Tones in a Commercial MRI Scanner: A Feasibility Study," M.S. thesis, Magnetic Resonance Research Center, Graz University of Technology, 2017. [Online]. Available: https://diglib.tugraz.at/download.php?id=5aa246a72fed9&location=browse

[3] A. C. Larson, R. D. White, G. Laub, E. R. McVeigh, D. Li, and O. P. Simonetti, "Self-gated cardiac cine MRI," *Magn. Reson. Med.*, vol. 51, no. 1, pp. 93–102, Jan. 2004, doi: 10.1002/mrm.10664.

[4] A. Pruitt *et al.*, "Fully self-gated whole-heart 4D flow imaging from a 5-minute scan," *Magn. Reson. Med.*, vol. 85, no. 3, pp. 1222–1236, Mar. 2021, doi: https://doi.org/10.1002/mrm.28491.

[5] P. Speier, M. Fenchel, and R. Rehner. PT-Nav: a novel respiratory navigation method for continuous acquisitions based on modulation of a pilot tone in the MR-receiver. In *Book of Abstracts ESMRMB 2015*, volume 28, pages S97–S98. Magnetic Resonance

Materials in Physics, Biology and Medicine, 2015. ISBN 09685243. doi: 10.1007/s10334-015-0488-1. URLhttp://link.springer. com/10.1007/s10334-015-0488-1.

[6] L. Schroeder, J. Wetzl, A. Maier, L. Lauer, J. Bollenbeck, M. Fenchel, and P. Speier. A Novel Method for Contact-Free Cardiac Synchronization Using the Pilot Tone Navigator. In *Proc. Intl. Soc. Mag. Reson. Med. 24*, page 0410, 2016. doi: 10.1002/mrm.25858.

[7] https://www.radiologie-muenchen.de/assets/upload/galerie/6787-cit13416-mr-magnetom-lumina-product-brochure-k5-hood05162002970357-final.pdf

[8] L. Schröder. *Information Content of a Novel MR Navigator Relating to Physiological Activities*. Master's thesis, Friedrich-Alexander-Universität Erlangen-Nürnberg, 2015.

[9] C. Chen *et al.*, "Extraction of cardiac and respiratory motion from Pilot Tone—a patient study". SCMR's Virtual Scientific Sessions 2021.

[10] P. Comon, "Independent component analysis, A new concept?," *Signal Processing*, vol. 36, no. 3, 1994, doi: 10.1016/0165-1684(94)90029-9.

[11] Feng *et al*., "XD-GRASP: Golden-angle radial MRI with reconstruction of extra motion-state dimensions using compressed sensing". *Magn. Reson. Med.* 2016;75(2):775-788.

[12] C. Chen, Y. Liu, O. P. Simonetti, and R. Ahmad, “Automatic Extraction and Sign Determination of Respiratory Signal in Real-Time Cardiac Magnetic Resonance Imaging,” 2020, pp. 1–4, doi: 10.1109/ISBI45749.2020.9098315.

[13] D. Kim, S. F. Cauley, K. S. Nayak, R. M. Leahy, and J. P. Haldar, “Region-optimized virtual (ROVir) coils: Localization and/or suppression of spatial regions using sensor-domain beamforming,” *Magn. Reson. Med.*, vol. 86, no. 1, 2021, doi: 10.1002/mrm.28706.